

*Supplementary Information*

**Polymer-grafted gold nanoflowers with temperature-controlled catalytic features by *in situ* particle growth and polymerization**

*Chaojian Chen,<sup>1,2</sup> David Yuen Wah Ng,<sup>1,\*</sup> and Tanja Weil<sup>1,2,\*</sup>*

<sup>1</sup>Max Planck Institute for Polymer Research, Ackermannweg 10, 55128 Mainz, Germany

<sup>2</sup>Ulm University, Albert-Einstein-Allee 11, 89081 Ulm, Germany

E-mails: weil@mpip-mainz.mpg.de; david.ng@mpip-mainz.mpg.de

**Table of Contents**

**I. EXPERIMENTAL**

- 1.1 Materials
- 1.2 Preparation of cationic HSA (cHSA)
- 1.3 Preparation of PEGylated cHSA (PEG-cHSA)
- 1.4 Synthesis of denatured PEG-cHSA (PEG-dcHSA)
- 1.5 Synthesis of macroinitiator PEG-dcHSA-Br
- 1.6 Preparation of PNIPAM-AuNFs
- 1.7 Catalytic reduction of *p*-nitrophenol

**II. CHARACTERIZATION**

- 2.1 Matrix-assisted laser desorption/ionization (MALDI) mass spectrometry
- 2.2 Transmission electron microscopy (TEM)
- 2.3 Dynamic light scattering (DLS)
- 2.4 UV-vis spectroscopy

### III. SUPPLEMENTARY RESULTS

**Fig. S1** MALDI-ToF mass spectrum of HSA

**Fig. S2** MALDI-ToF mass spectrum of cHSA

**Fig. S3** MALDI-ToF mass spectrum of PEG-cHSA

**Fig. S4** MALDI-ToF mass spectrum of PEG-dcHSA

**Fig. S5** MALDI-ToF mass spectrum of PEG-dcHSA-Br

**Fig. S6** TEM characterization of PNIPAM-AuNFs entry 1

**Fig. S7** TEM characterization of PNIPAM-AuNFs entry 2

**Fig. S8** TEM characterization of PNIPAM-AuNFs entry 3

**Fig. S9** TEM characterization of PNIPAM-AuNFs entry 4

**Fig. S10** TEM characterization of PNIPAM-AuNFs entry 5

**Fig. S11** TEM characterization of PNIPAM-AuNFs entry 6

**Fig. S12** DLS measurements of PNIPAM-AuNFs under different temperatures

**Fig. S13** UV-vis spectrum for the mixture of NaBH<sub>4</sub> and *p*-nitrophenol aqueous solution without adding PNIPAM-AuNFs after mixing 2 h.

**Fig. S14** Conversion *versus* reaction time for the reduction of *p*-nitrophenol using PNIPAM-AuNFs as the catalyst at different temperatures.

**Fig. S15** Catalytic performance of recycled PNIPAM-AuNFs (entry 4) for the hydrogenation reaction.

**Table S1** Sizes of PNIPAM-AuNFs (entry 4) at different temperatures determined by DLS

**Table S2** Comparison of catalytic activities of various gold catalysts for the reduction of *p*-nitrophenol.

### IV. REFERENCES

## I. EXPERIMENTAL

### 1.1 Materials

Human serum albumin (HSA, 96%), tris(2-carboxyethyl) phosphine hydrochloride (TCEP,  $\geq 98\%$ ), 2-bromoisobutanoic acid *N*-hydroxysuccinimide ester (NHS-BiB, 98%), *O*-[(*N*-succinimidyl)succinyl-aminoethyl]-*O'*-methylpolyethylene glycol (NHS-PEG,  $M_n \sim 2000$ ), *N*-(2-aminoethyl)maleimide trifluoroacetate salt (MI-NH<sub>2</sub>, 95%), *N*-(3-Dimethylaminopropyl)-*N'*-ethylcarbodiimide hydrochloride (EDC·HCl,  $\geq 98\%$ ), tris(2-pyridylmethyl)amine (TPMA, 98%), copper(II) bromide (CuBr<sub>2</sub>, 99%), *p*-nitrophenol ( $\geq 99\%$ ), and L-ascorbic acid ( $\geq 99\%$ ) were purchased from Sigma-Aldrich and used without further treatment. Chloroauric acid (HAuCl<sub>4</sub>,  $>99.5\%$ ) was obtained from Carl Roth. Ethylenediamine ( $>99\%$ ), urea (99.5%) and ethylenediaminetetraacetic acid (EDTA, 98%) were purchased from Acros Organics and used as received. *N*-isopropylacrylamide (NIPAM,  $>98\%$ ) was bought from TCI. Sodium borohydride (NaBH<sub>4</sub>,  $>95\%$ ) was obtained from Fisher Chemical. All other solvents and salts were obtained from commercial suppliers and used as received.

### 1.2 Preparation of cationic HSA (cHSA) <sup>[1]</sup>

HSA (150 mg, 2.26  $\mu$ mol) was dissolved in 15 mL of degassed ethylenediamine solution (2.5 M) and the pH was tuned to 4.75 with HCl. After adding EDC·HCl (4 mmol, 766 mg) and stirring for two hours at room temperature, acetate buffer (1 mL, 4 M, pH 4.75) was added to terminate the reaction. The obtained reaction solution was purified twice with acetate buffer (100 mM, pH 4.75) and three times with deionized water by ultracentrifugation using a Vivaspin 20 concentrator (MWCO 30 kDa). The resulting solution was lyophilized to afford the product as a white fluffy solid (154 mg, yield: 94%, MALDI-ToF MS: 72.3 kDa).

### 1.3 Preparation of PEGylated cHSA (PEG-cHSA) <sup>[1]</sup>

First, cHSA (100 mg, 1.4  $\mu$ mol) was dissolved in degassed phosphate buffer (30 mL, 50 mM, pH 8.0). NHS-PEG (105 mg, 52.4  $\mu$ mol) was dissolved in 0.4 mL of DMSO and then added to the cHSA solution. After stirring at room temperature for four hours, the reaction solution was purified five times with deionized water by ultracentrifugation using a Vivaspin

20 concentrator (MWCO 30 kDa). The resulting solution was lyophilized to obtain the product as a white fluffy solid (151 mg, yield: 80 %). The MALDI-ToF MS indicated a molecular weight of 136.6 kDa which means on average 32 PEG chains were conjugated to each cHSA backbone.

#### **1.4 Synthesis of denatured PEG-cHSA (PEG-dcHSA) <sup>[2]</sup>**

##### *Preparation of the urea-phosphate buffer (urea-PB)*

Urea (150.15 g, 2.5 mol), EDTA (292.24 mg, 1 mmol), Na<sub>2</sub>HPO<sub>4</sub>·7H<sub>2</sub>O (5.4276 g, 25 mmol) and NaH<sub>2</sub>PO<sub>4</sub> (0.5699 g, 25 mmol) were dissolved in 0.5 L of deionized water. The urea-PB with 50 mM phosphate buffer, 5 M urea and 2 mM EDTA was then obtained by adjusting the pH to 7.4.

##### *Synthesis of PEG-dcHSA*

To a 50 mL flask, 20 mL of urea-PB was added and then degassed via bubbling for five minutes. Followed PEG-cHSA (27.2 mg, 200 nmol) was dissolved and further stirred for 15 min. TCEP (0.58 mg, 2 μmol) was added and stirred for 30 min under argon flow. Lastly, MI-NH<sub>2</sub> (15.24 mg, 60 μmol) was added and stirred overnight under argon protection. The obtained reaction solution was purified three times with urea-PB and five times with deionized water by ultracentrifugation using a Vivaspin 20 concentrator (MWCO 30 kDa). The resulting solution was lyophilized to afford the product as a white fluffy solid (24.1 mg, yield: 86%, MALDI-ToF MS: 140.4 kDa).

#### **1.5 Synthesis of macroinitiator PEG-dcHSA-Br**

PEG-dcHSA-Br was synthesized by attaching ATRP initiators to PEG-dcHSA. In a typical procedure, PEG-dcHSA (20 mg, 145 nmol) was dissolved in 20 mL of NaHCO<sub>3</sub> (0.1 M, pH 8.5). NHS-BiB (218 mg, 0.826 mmol) dissolved in 2.18 mL of DMSO was then added dropwise into the PEG-dcHSA solution. The reaction solution was stirred overnight at room temperature and purified eight times with deionized water by ultracentrifugation using a Vivaspin 20 concentrator (MWCO 50 kDa). The product was obtained as a white fluffy solid after lyophilizing (11.1 mg, yield: 51%, MALDI-ToF MS: 149.5 kDa).

## 1.6 Preparation of PNIPAM-AuNFs

### Preparation of the stock solution of CuBr<sub>2</sub>/TPMA catalyst

CuBr<sub>2</sub> (4.47 mg, 0.02 mmol) and TPMA (46.5 mg, 0.16 mmol) was dissolved in 1 mL mixed solution of water:DMF (1:1 v/v) and stored at 4 °C prior to use. Therefore, the concentration of the effective Cu<sup>2+</sup> in the stock solution was 20 nmol μL<sup>-1</sup>.

### Preparation of the ascorbic acid solution

To a 10 mL Schlenk flask, L-ascorbic acid (4.4 mg, 25 μmol) was firstly added under argon flow. Degassed deionized water (5 mL) was then added to dissolve L-ascorbic acid. The solution was then stirred under argon flow for 40 min. Therefore, the concentration of L-ascorbic acid was 5 nmol μL<sup>-1</sup>.

### Synthesis of PNIPAM-AuNFs

In a typical procedure for the synthesis of PNIPAM-AuNFs (Entry 1 in Table 1), the protein-derived substrate and macroinitiator PEG-dcHSA-Br (0.449 mg, 3 nmol with ~300 nmol of amino groups and 183 nmol of ATRP initiation sites) was first dissolved in Milli-Q water with a concentration of 1 mg mL<sup>-1</sup> and then added into a 5 mL Schlenk tube. Followed HAuCl<sub>4</sub> solution (25 μL, 2 mM in Milli-Q water), the monomer NIPAM (41.4 mg, 366 μmol), the stock solution of Cu<sup>II</sup>Br<sub>2</sub>/TPMA catalyst (11 μL, 220 nmol of Cu<sup>2+</sup>), and 0.55 mL of Milli-Q water were added. Oxygen in the mixture was then removed through three freeze-pump-thaw cycles and the solution was stirred at room temperature for one hour for the gold ions to absorb to the amino groups of PEG-dcHSA-Br. Ascorbic acid solution was then added via a syringe pump at a slow speed of 0.6 μL min<sup>-1</sup>, the reaction was proceeded for 2 h at room temperature (23 °C). The final product was purified by centrifugation to remove the unreacted monomers and other impurities. For Entry 2 and 3, the molar ratio of amino groups from PEG-dcHSA-Br to HAuCl<sub>4</sub> was tuned by increasing the added amount of HAuCl<sub>4</sub>. For other reaction conditions (Entry 4-6), the reaction temperature and time were changed respectively.

### 1.7 Catalytic reduction of *p*-nitrophenol

1 mL of NaBH<sub>4</sub> aqueous solution (50 mM dissolved in Milli-Q water) and 0.2 mL of freshly prepared *p*-nitrophenol aqueous solution (1 mM, pH = 12) were added to a 2 mL cuvette and mixed. The cuvette was placed in a water bath at a determined temperature. Then, 0.1 mL of PNIPAM-AuNFs solution with 0.01 μmol (1.97 μg) Au was quickly injected into the reaction cuvette and the reaction was monitored by UV-vis spectrometer. The absorbance at 400 nm was subtracted from that at 500 nm to correct for background absorption and then used to calculate the conversion and apparent rate constant ( $k_{app}$ ). The conversion ( $C$ ) was calculated using the following equation

$$C = \frac{A_0 - A_t}{A_0} \times 100\%$$

where  $A_0$  and  $A_t$  are the absorbance at time 0 and  $t$ . The apparent rate constant was determined as the slope of  $\ln(A_0/A_t)$  at 400 nm against to the reaction time.

## **II. CHARACTERIZATION**

### **2.1 Matrix-assisted laser desorption/ionization (MALDI) mass spectrometry**

MALDI time-of-flight (MALDI-ToF) mass spectrometry was performed on Bruker rapifleX spectrometer. Saturated solution of sinapinic acid dissolved in a 50:50 water/acetonitrile with 0.2% TFA (trifluoroacetic acid) was used as the matrix solution.

### **2.2 Transmission electron microscopy (TEM)**

TEM samples were prepared by adding 4  $\mu\text{L}$  of the PNIPAM-AuNFs solution onto a carbon-coated copper grid. After drying in air for 10 min, the remained solution was removed by a filter paper and the grid was then dried in air. The measurement was conducted on a JEOL JEM-1400 TEM operating at an accelerating voltage of 120 kV. ImageJ software was used for the analysis of the size of PNIPAM-AuNFs samples.

### **2.3 Dynamic light scattering (DLS)**

The aqueous solution of PNIPAM-AuNFs was filtered through a 0.5  $\mu\text{m}$  filter (Millipore LCR) into a cylindrical quartz cuvette (18 mm diameter, Hellma, Germany) after cleaning it in an acetone fountain to remove dust. The experiment was performed on an ALV spectrometer (ALV-GmbH, Germany) equipped with an He-Ne laser ( $\lambda = 632.8 \text{ nm}$ ). For temperature-controlled measurements, the light scattering instrument was equipped with a thermostat from Julabo. All experiments were performed as a triplicate measurement. Data analysis was performed using ALV5000 software.

### **2.4 UV-vis spectroscopy**

The samples were added in a Greiner 96 flat transparent plate. UV-vis absorbance spectra were collected using a TECAN (Spark 20M) microplate reader. The wavelength range was set from 250 to 500 nm. Before measurement, the plate was shaken for three seconds with a shaking amplitude of 1 mm and frequency of 1440 rpm.

### III. SUPPLEMENTARY RESULTS

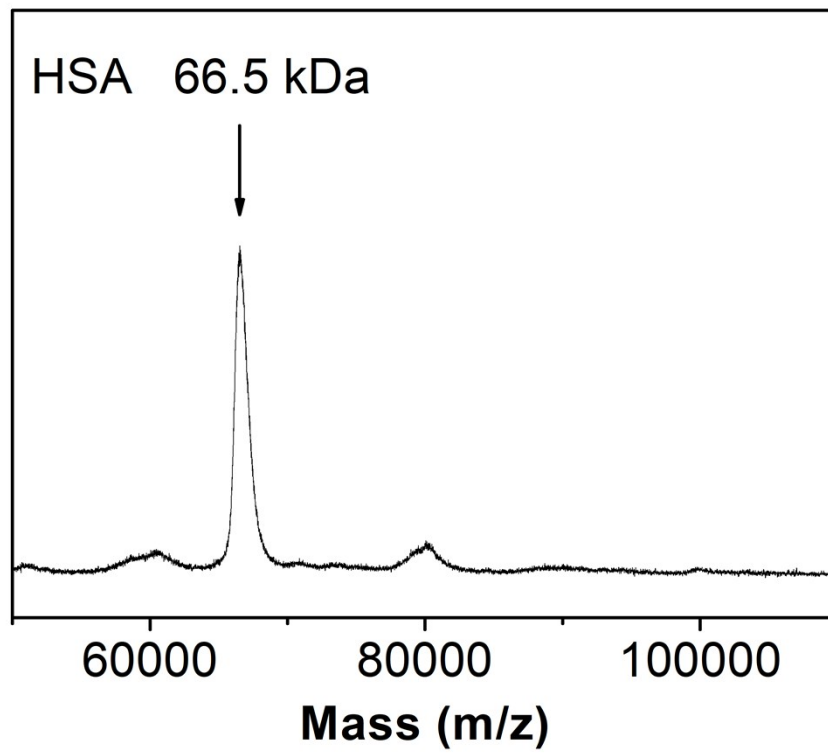


Fig. S1 MALDI-ToF mass spectrum of HSA.



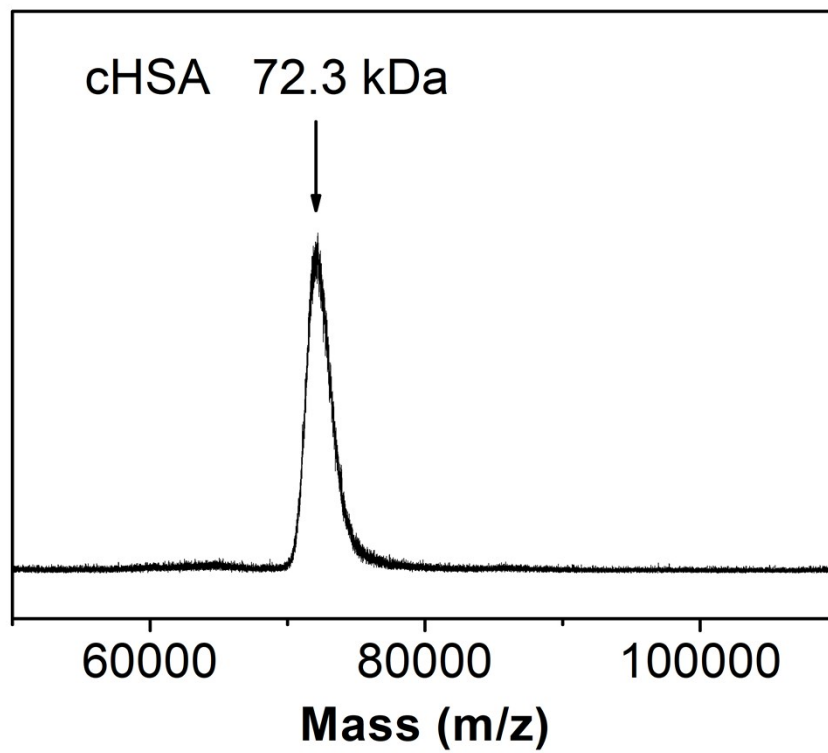


Fig. S2 MALDI-ToF mass spectrum of cHSA.

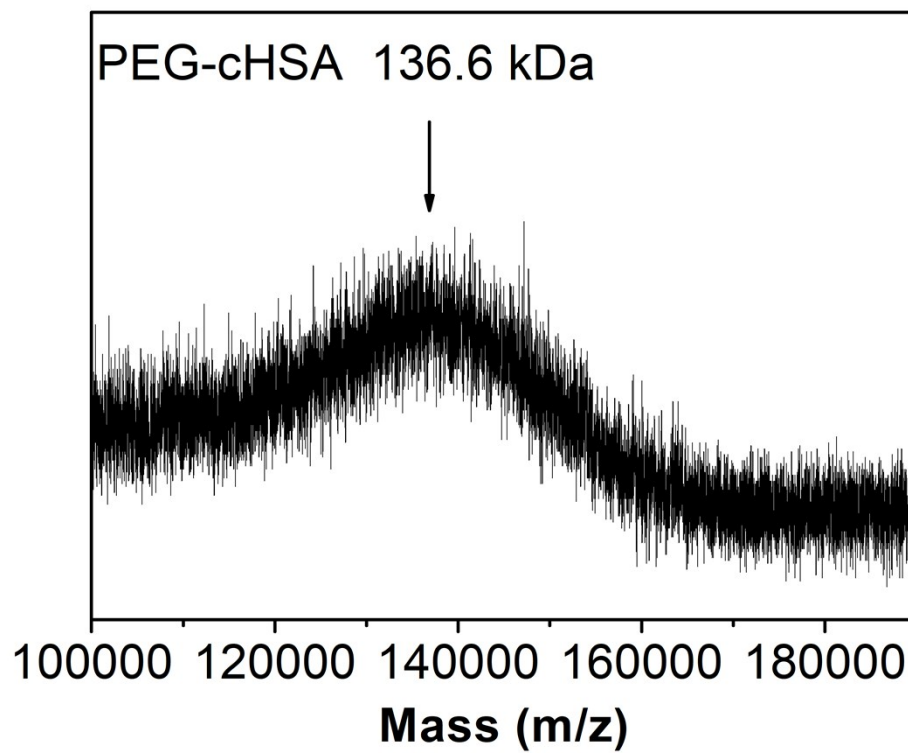


Fig. S3 MALDI-ToF mass spectrum of PEG-cHSA.

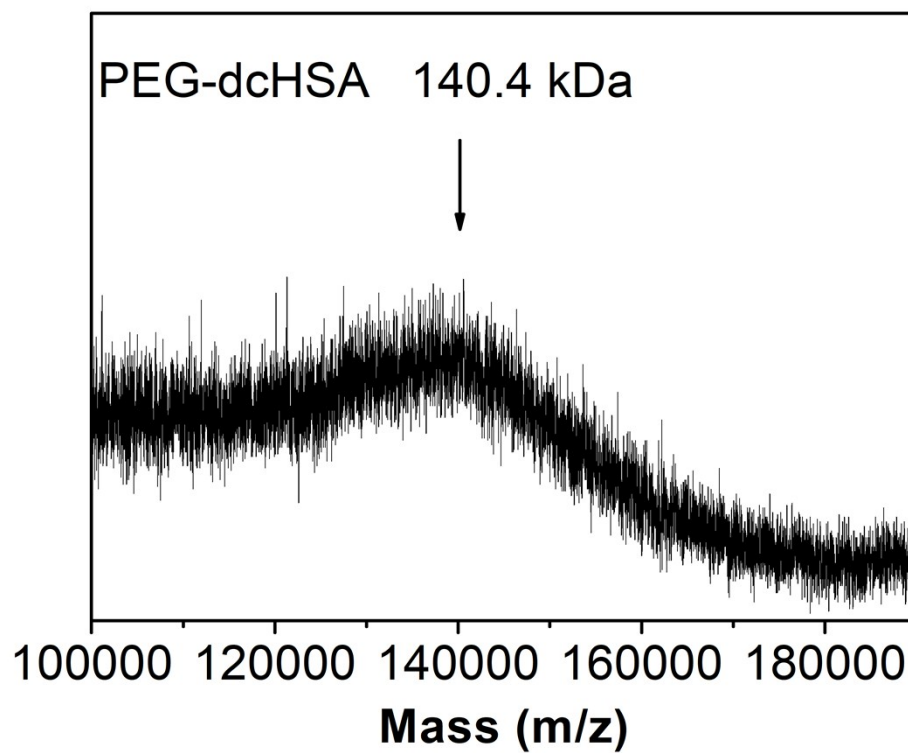


Fig. S4 MALDI-ToF mass spectrum of PEG-dcHSA.

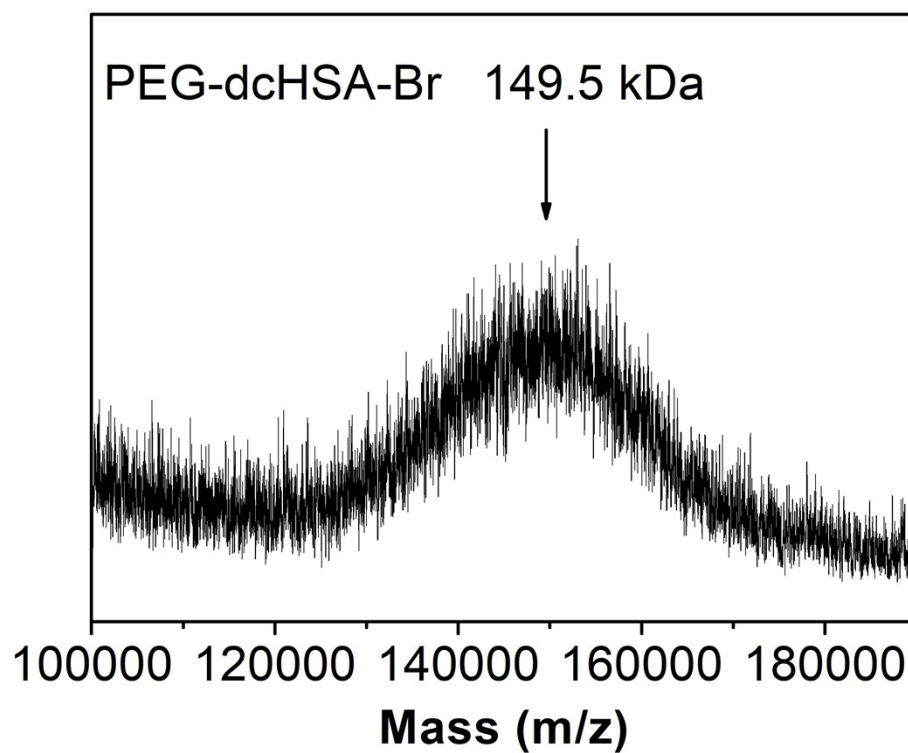
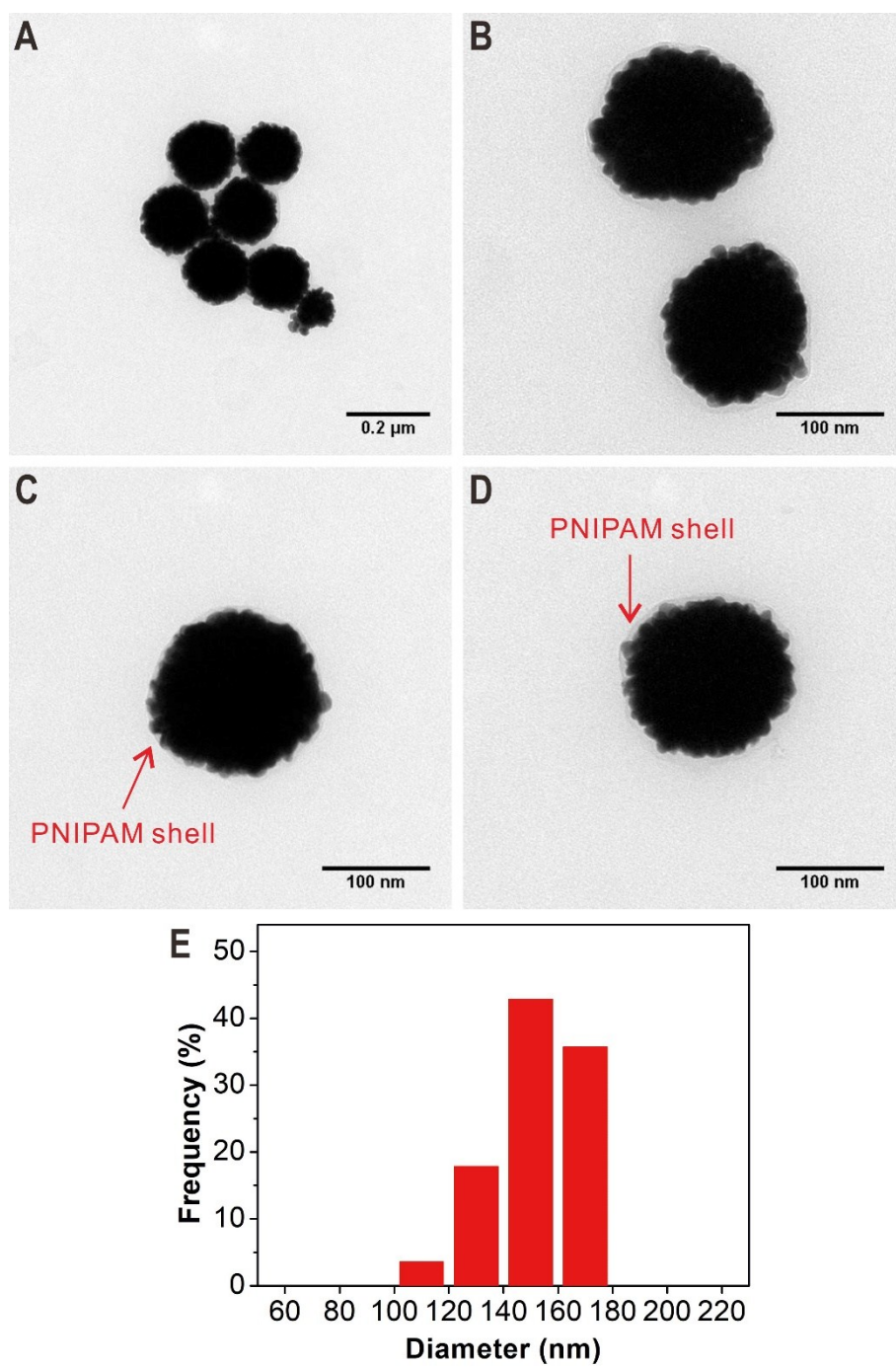
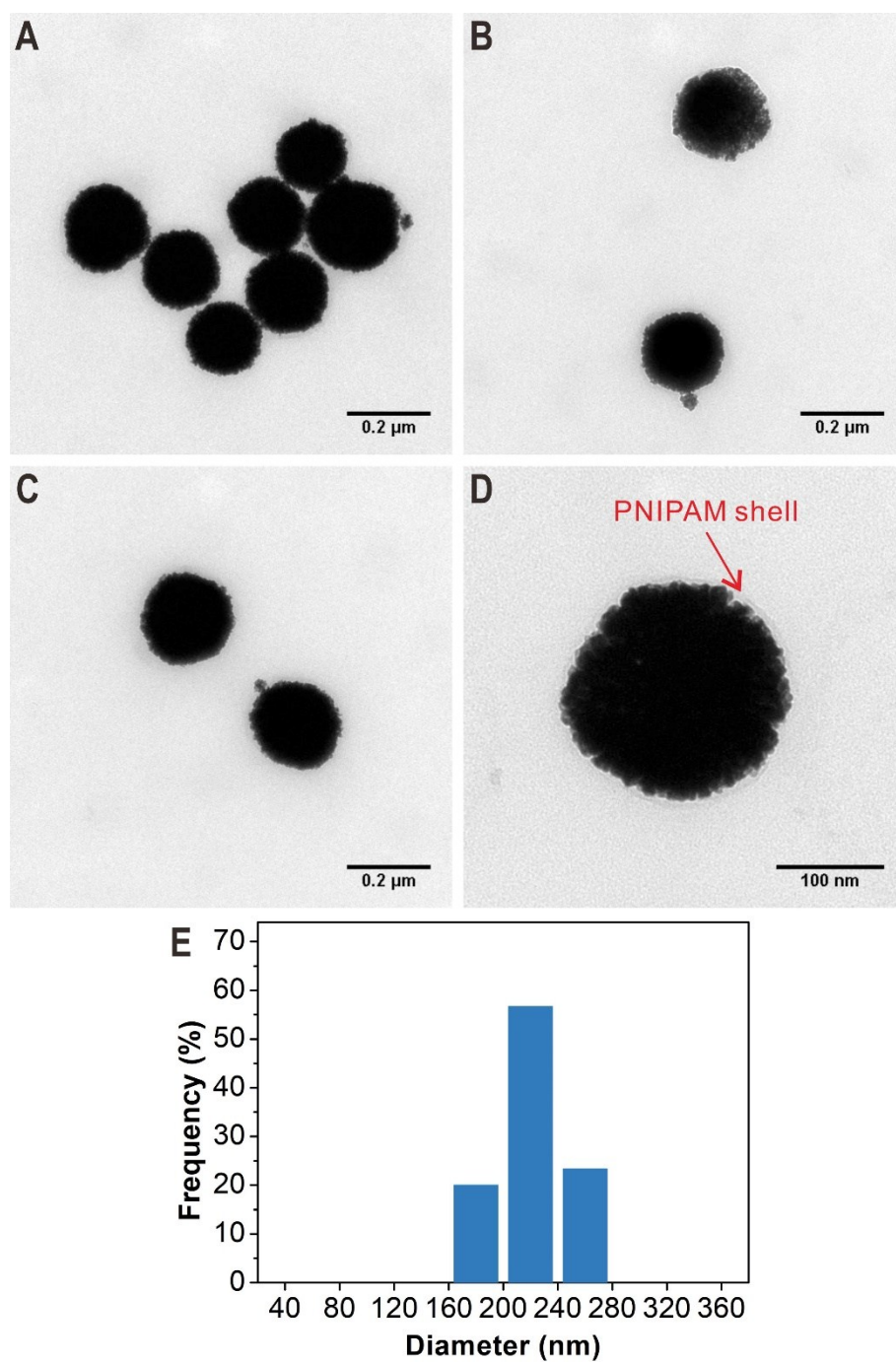


Fig. S5 MALDI-ToF mass spectrum of PEG-dcHSA-Br.



**Fig. S6** TEM images (A-D) and size distribution (E) of PNIPAM-AuNFs entry 1 in Table 1 prepared with a molar ratio of  $-\text{NH}_2/\text{HAuCl}_4 = 6:1$  at 23  $^\circ\text{C}$  for 2 h.



**Fig. S7** TEM images (A-D) and size distribution (E) of PNIPAM-AuNFs entry 2 in Table 1 prepared with a molar ratio of  $-\text{NH}_2/\text{HAuCl}_4 = 3:1$  at 23  $^\circ\text{C}$  for 2 h.

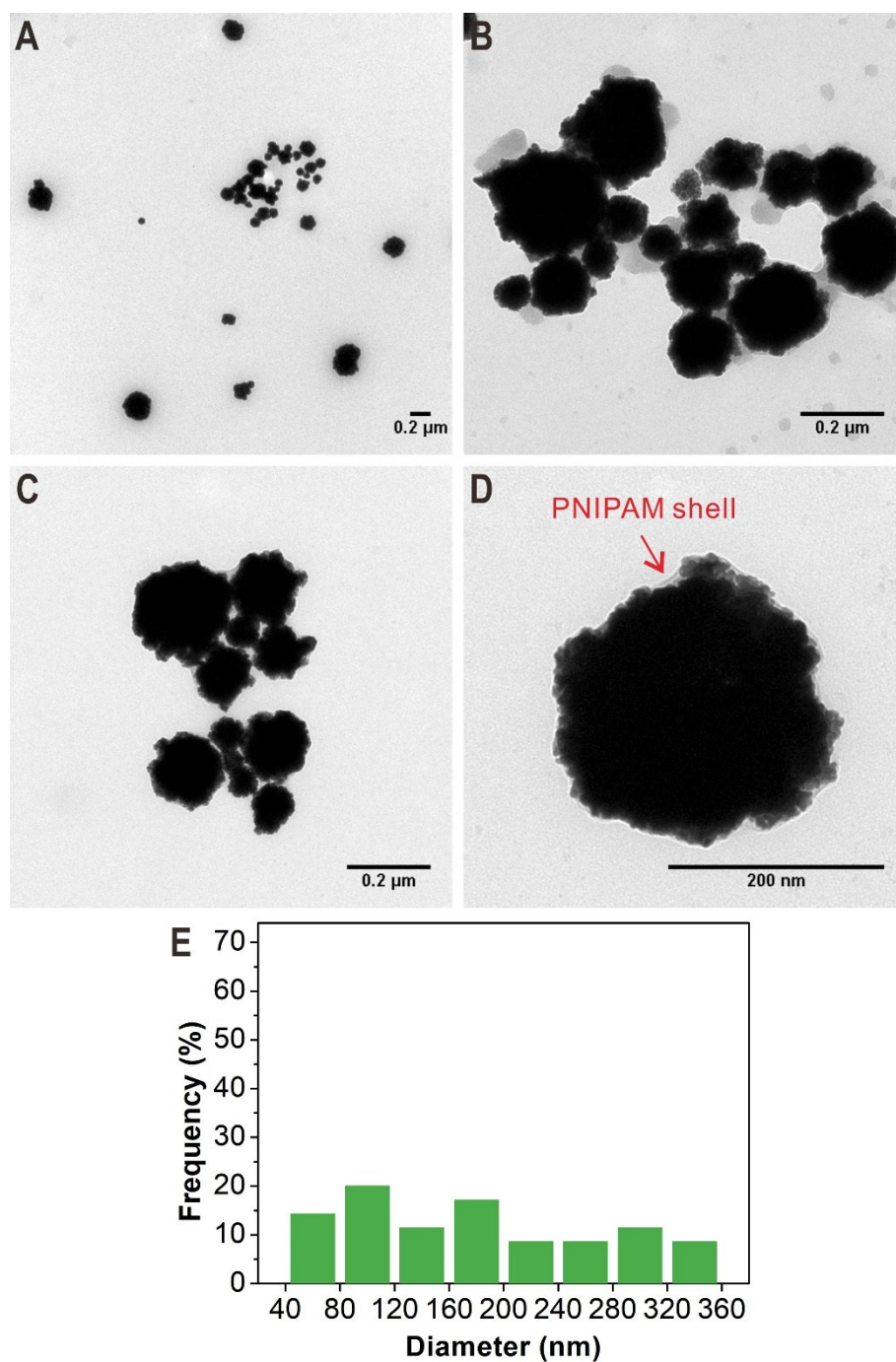


**Fig. S8** TEM images (A-D) and size distribution (E) of PNIPAM-AuNFs entry 3 in Table 1 prepared with a molar ratio of  $-\text{NH}_2/\text{HAuCl}_4 = 1:1$  at 23  $^\circ\text{C}$  for 2 h.



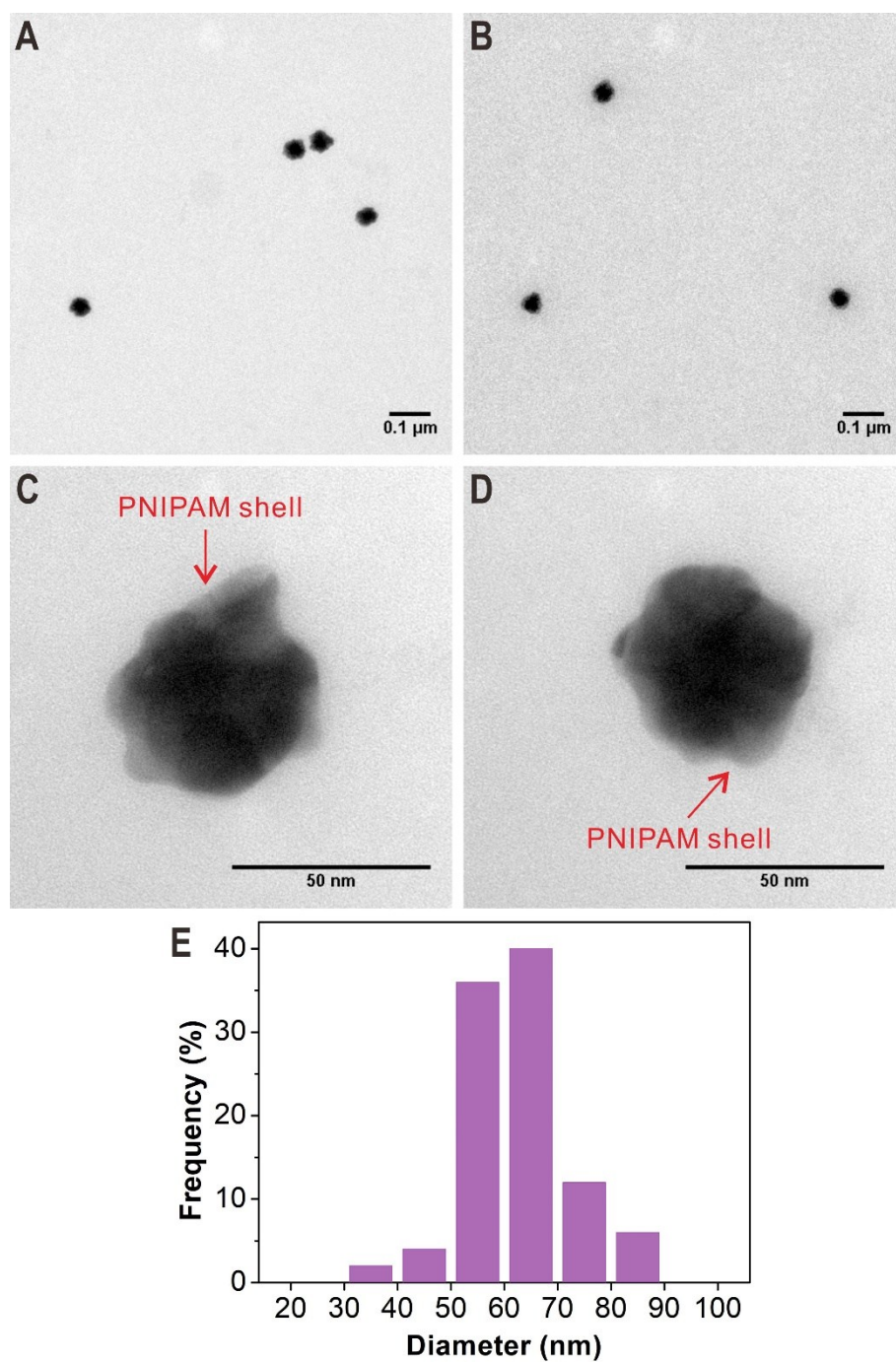


**Fig. S9** TEM images (A-D) and size distribution (E) of PNIPAM-AuNFs entry 4 in Table 1 prepared with a molar ratio of  $\text{-NH}_2/\text{HAuCl}_4 = 3:1$  at 40 °C for 2 h.

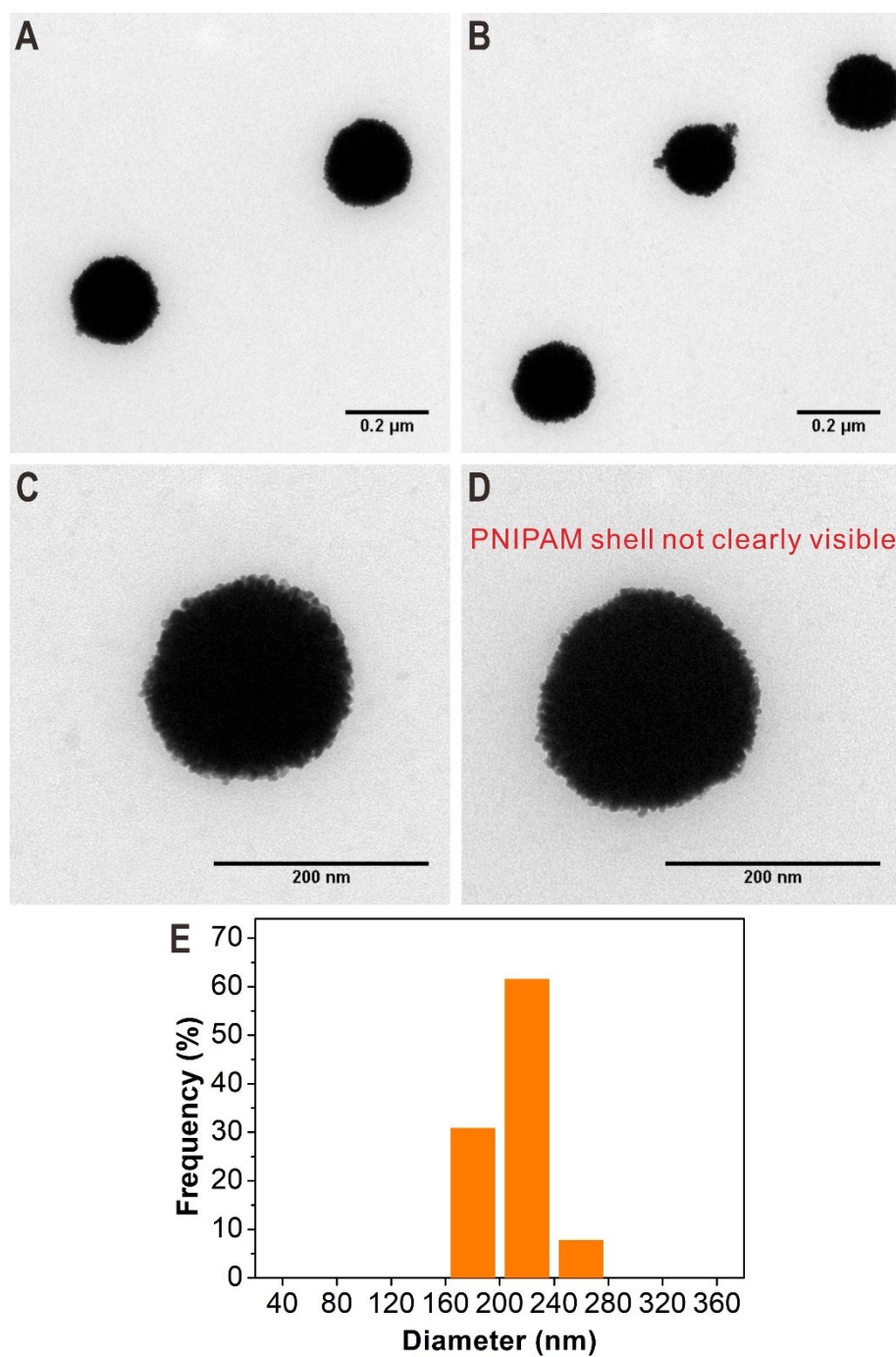


**Fig. S10** TEM images (A-D) and size distribution (E) of PNIPAM-AuNFs entry 5 in Table 1 prepared with a molar ratio of  $-\text{NH}_2/\text{HAuCl}_4 = 3:1$  at 23  $^\circ\text{C}$  for 1 h.

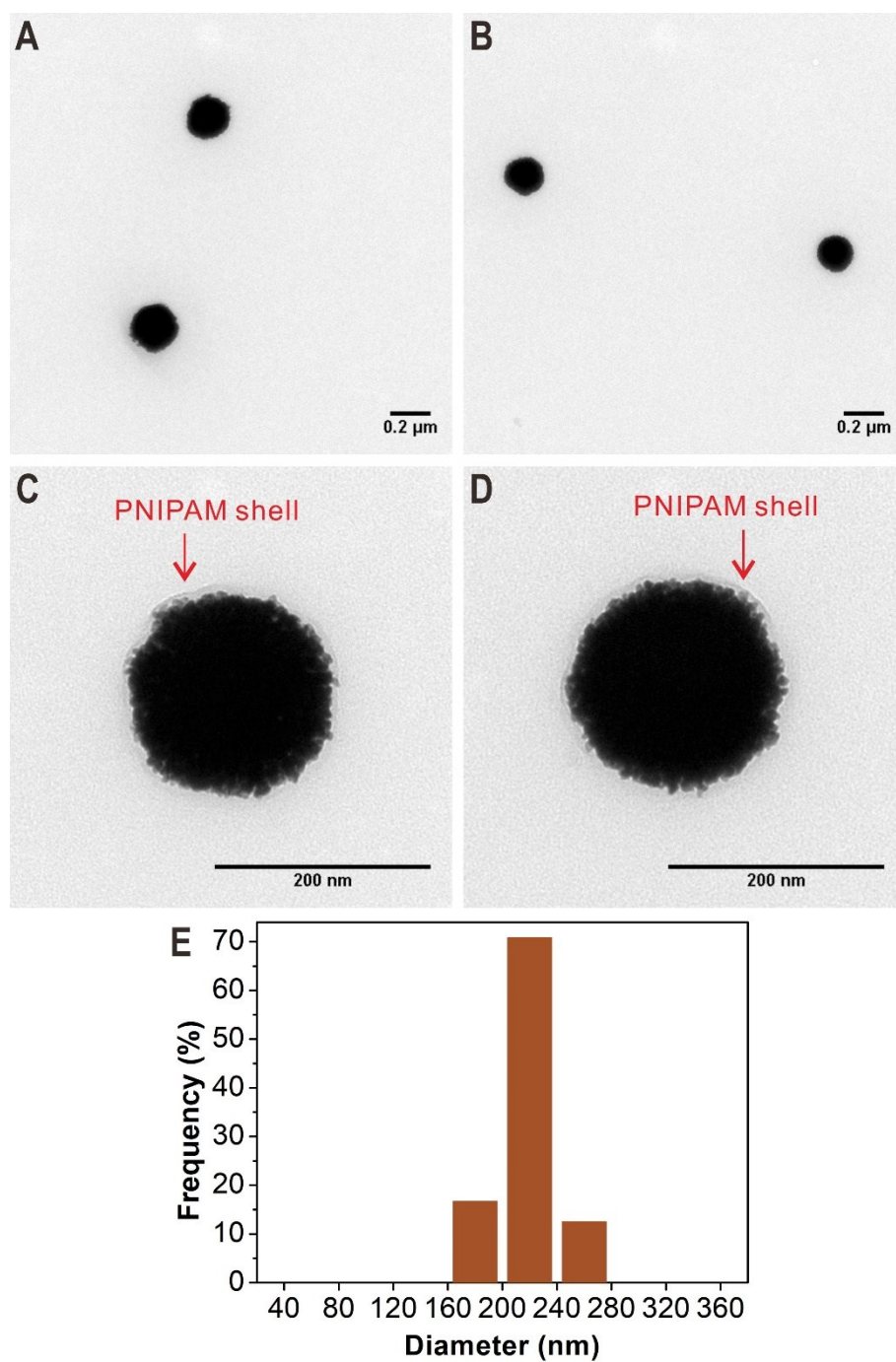


**Fig. S11** TEM images (A-D) and size distribution (E) of PNIPAM-AuNFs entry 6 in Table 1 prepared with a molar ratio of  $\text{-NH}_2/\text{HAuCl}_4 = 3:1$  at 23 °C for 4 h.



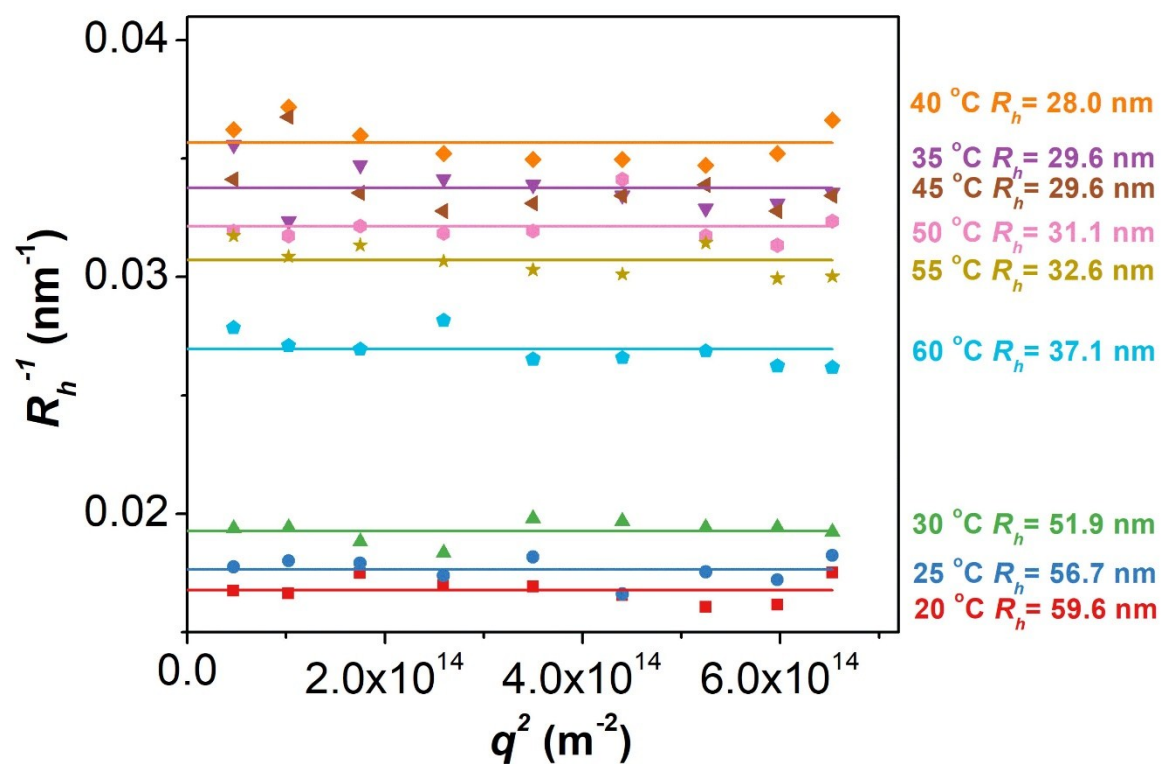


Fig. S12 DLS measurement of PNIPAM-AuNFs (entry 4 prepared under 40 °C) by tuning the temperature from 20 °C to 60 °C with a step of 5 °C.

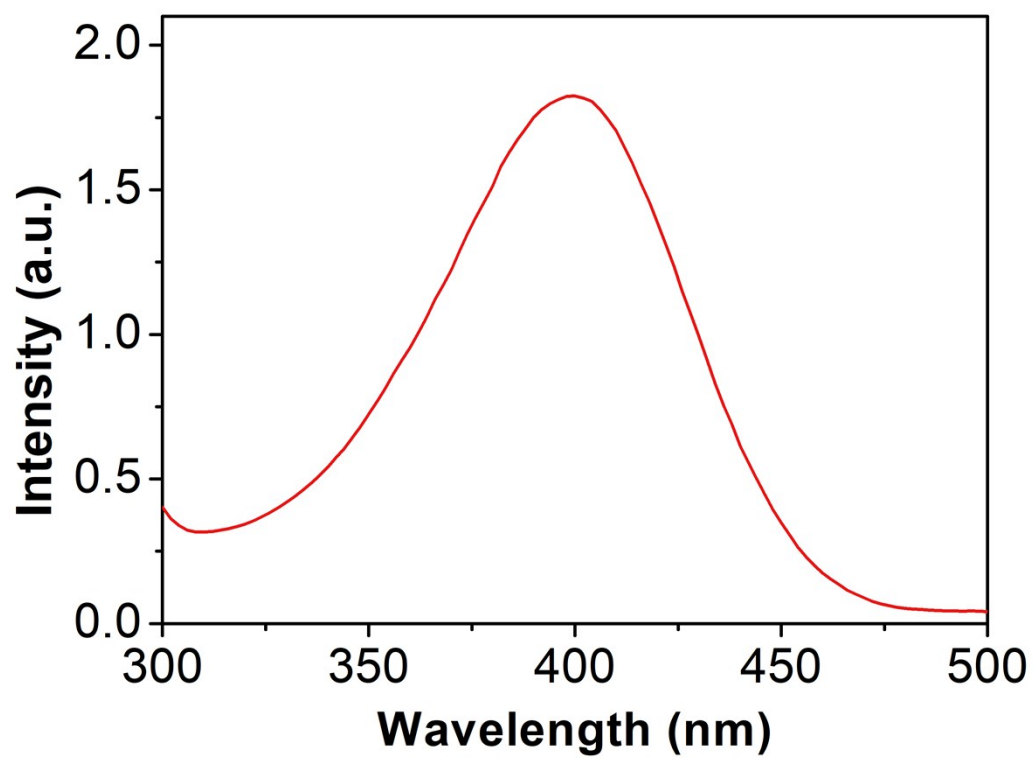


Fig. S13 UV-vis spectrum for the mixture of  $\text{NaBH}_4$  and *p*-nitrophenol aqueous solution without adding PNIPAM-AuNFs after mixing 2 h.

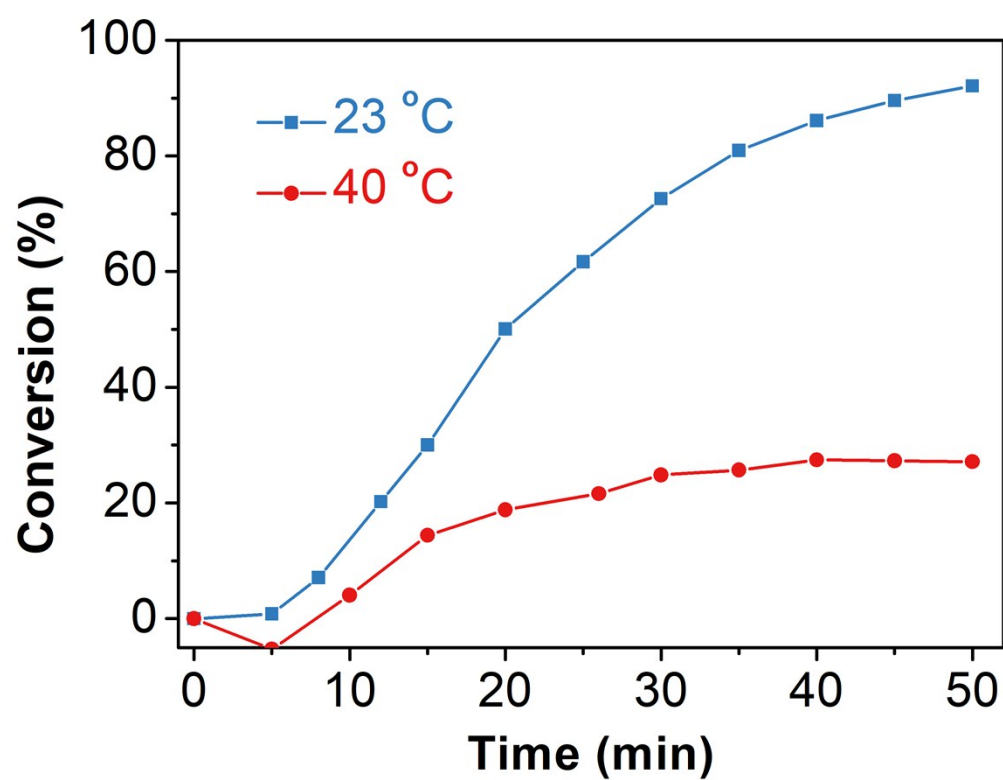
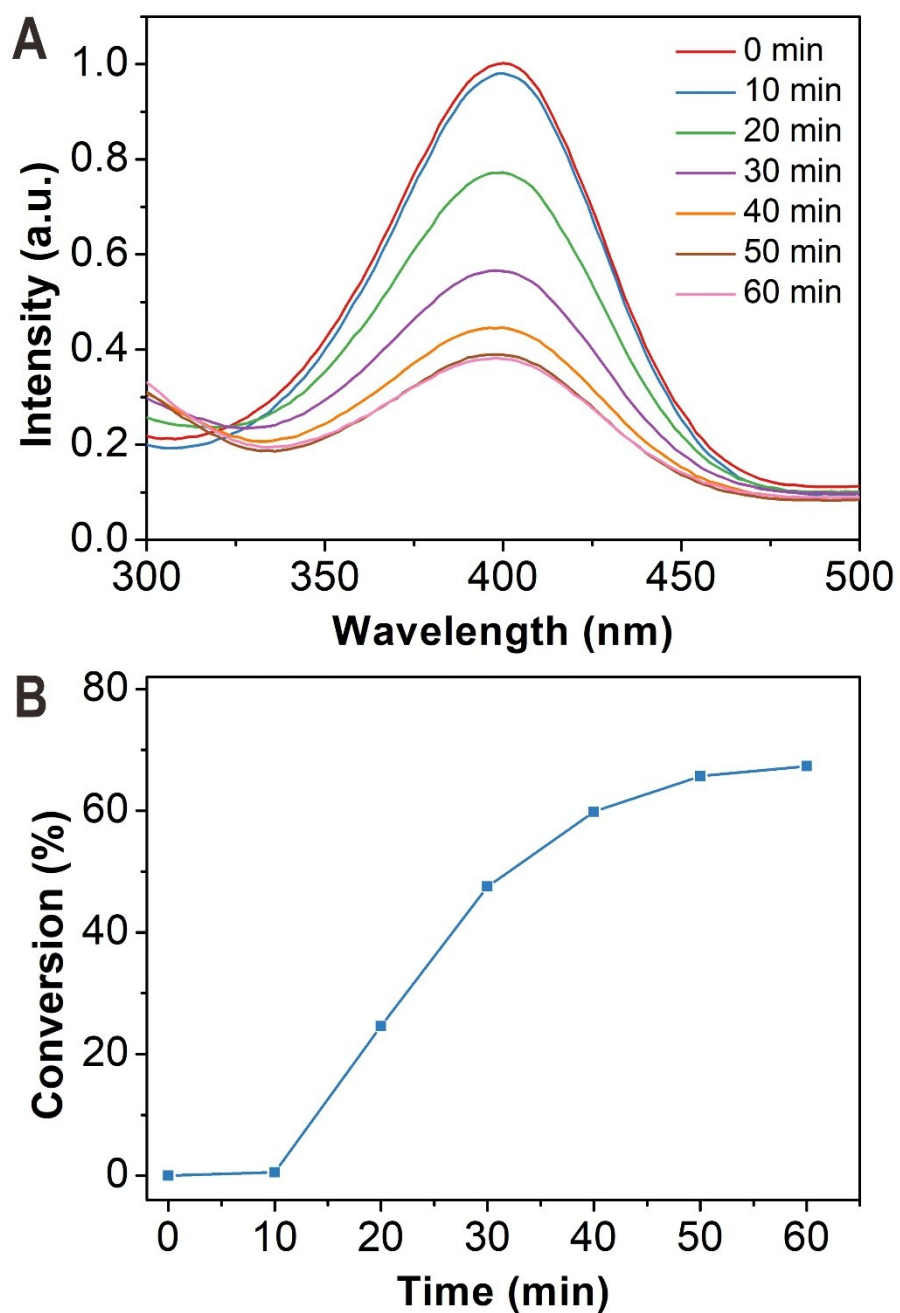


Fig. S14 Conversion *versus* reaction time for the reduction of *p*-nitrophenol using PNIPAM-AuNFs as the catalyst at different temperatures.



**Fig. S15** Catalytic performance of recycled PNIPAM-AuNFs (entry **4**) for the hydrogenation reaction. (A) UV-vis spectra of the reaction solution for the hydrogenation of *p*-nitrophenol at different time points at room temperature. (B) Conversion *versus* reaction time for the reduction reaction catalyzed by the recycled PNIPAM-AuNFs.

**Table S1** Sizes of PNIPAM-AuNFs (entry **4**) at different temperatures determined by DLS.

temperature (°C)	20	25	30	35	40	45	50	55	60
$R_h$ (nm)	59.6	56.7	51.9	29.6	28	29.6	31.1	32.6	37.1

**Table S2** Comparison of catalytic activities of various gold catalysts for the reduction of *p*-nitrophenol.

Au-based catalysts	$k_{app}$ ( $\times 10^{-3} \text{ s}^{-1}$ )	$m_{Au}$	$k_{app}/m_{Au}$ ( $\text{s}^{-1} \text{ g}^{-1}$ )	$M_{Au}$ ( $\text{mg L}^{-1}$ )	$k_{app}/M_{Au}$ ( $\times 10^{-3} \text{ L s}^{-1} \text{ mg}^{-1}$ )	activity tunability	refs
PNIPAM-AuNFs	1.02	1.97 $\mu\text{g}$	518	1.52	0.67	YES	this work
Au meso-flowers	/	/	1.56	/	/	NO	[3]
AuNFs	0.65	0.2 mg	3.25	62.5	0.01	NO	[4]
Spongy Au nanocrystals	2.1	6 mg	0.35	2000	0.001	NO	[5]
Au sponges	5.0	3 mg	1.67	274	0.018	NO	[6]
Hollow AuNFs	24.4	/	/	8	3.05	NO	[7]
Au nanospheres	/	/	/	/	0.462	NO	[7]
Au NPs@porous films	6.3	1.75 mg	3.6	88	0.072	NO	[8]
Au NPs@fiber	6-8	0.43 mg	14.0-18.6	8.6	0.70-0.93	NO	[9]
Au NPs@hydrogel	1.1	12 $\mu\text{g}$	91.7	3.87	0.28	YES	[10]
Flower-like Au nanochains	0.783	0.2 mg	3.92	62.5	0.013	NO	[11]

$k_{app}$ : apparent rate constant

$m_{Au}$ : amount of Au

$M_{Au}$ : concentration of Au

/ = not mentioned

#### IV. REFERENCES

- [1] Y. Z. Wu, S. Ihme, M. Feuring-Buske, S. L. Kuan, K. Eisele, M. Lamla, Y. R. Wang, C. Buske, T. Weil, *Adv. Healthc. Mater.* **2013**, 2, 884-894.
- [2] Y. Z. Wu, A. Ermakova, W. N. Liu, G. Pramanik, T. M. Vu, A. Kurz, L. McGuinness, B. Naydenov, S. Hafner, R. Reuter, J. Wrachtrup, J. Isoya, C. Fortsch, H. Barth, T. Simmet, F. Jelezko, T. Weil, *Adv. Funct. Mater.* **2015**, 25, 6576-6585.
- [3] H. Z. Zou, G. H. Ren, M. Y. Shang, W. Q. Wang, *Mater. Chem. Phys.* **2016**, 176, 115-120.
- [4] A. J. Wang, Y. F. Li, M. Wen, G. Yang, J. J. Feng, J. Yang, H. Y. Wang, *New J. Chem.* **2012**, 36, 2286-2291.
- [5] M. H. Rashid, R. R. Bhattacharjee, A. Kotal, T. K. Mandal, *Langmuir* **2006**, 22, 7141-7143.
- [6] Y. Yu, W. Q. Xiao, T. T. Zhou, P. Zhang, C. Yan, Z. J. Zheng, *Mater. Chem. Front.* **2017**, 1, 482-486.
- [7] S. J. Ye, F. Benz, M. C. Wheeler, J. Oram, J. J. Baumberg, O. Cespedes, H. K. Christenson, P. L. Coletta, L. J. C. Jeuken, A. F. Markham, K. Critchley, S. D. Evans, *Nanoscale* **2016**, 8, 14932-14942.
- [8] Y. L. Ye, M. Jin, D. C. Wan, *J Mater. Chem. A* **2015**, 3, 13519-13525.
- [9] M. L. Wang, T. T. Jiang, Y. Lu, H. J. Liu, Y. Chen, *J Mater. Chem. A* **2013**, 1, 5923-5933.
- [10] G. Marcelo, M. Lopez-Gonzalez, F. Mendicuti, M. P. Tarazona, M. Valiente, *Macromolecules* **2014**, 47, 6028-6036.
- [11] A. J. Wang, S. F. Qin, D. L. Zhou, L. Y. Cai, J. R. Chen, J. J. Feng, *RSC Adv.* **2013**, 3, 14766-14773.